



UKAEA

Preprint

MEASUREMENT OF MAGNETIC FIELDS IN A TOKAMAK USING LASER LIGHT SCATTERING

M J FORREST
P G CAROLAN
N J PEACOCK

CULHAM LABORATORY
Abingdon Oxfordshire

1977

This document is intended for publication in a journal or at a conference and is made available on the understanding that extracts or references will not be published prior to publication of the original, without the consent of the authors.

Enquiries about copyright and reproduction should be addressed to the Librarian, UKAEA, Culham Laboratory, Abingdon, Oxfordshire, England

MEASUREMENT OF MAGNETIC FIELDS IN A TOKAMAK USING LASER LIGHT SCATTERING

M.J. Forrest, P.G. Carolan, N.J. Peacock

Culham Laboratory, Abingdon, Oxon, OX14 3DB, UK
(Euratom/UKAEA Fusion Association)

A B S T R A C T

Measurement of the local magnetic fields in a TOKAMAK plasma has been demonstrated by laser light scattering from the free electrons. The technique, which does not disturb the plasma conditions, exploits the sensitivity of the cyclotron modulation of the scattered light spectrum to the angle between the local magnetic field and the plane in which the scattered light is observed.

Theoretical constraints for observation of the modulated light spectrum are shown to be satisfied in the experiment. In practice, sufficient accuracy is achieved to derive the detailed volume current distribution - an essential factor in the energy balance and in plasma stability. The method may be applied to the considerably larger fusion research facilities currently envisaged.

(Submitted for publication in Nature)

INTRODUCTION

In controlled fusion devices such as TOKAMAKS with strong magnetic fields, the gross stability and equilibrium of the plasma is governed by the pitch angle of the force lines (Shafranov⁽¹⁾). The strong toroidal field, B_ϕ , combined with the relatively weak self field, B_θ , due to axially driven heating currents, as shown in Fig. 1a, can provide a stable configuration for the plasma.

It is the purpose of this paper to report on measurements of the distribution of field directions from which the poloidal field distribution, $B_\theta(r)$, can be calculated. The equilibrium and stability behaviour of the plasma can then be studied in terms of the stability factor $q^{(1)}$ ($q(r) = \frac{r}{R} \frac{B_\phi}{B_\theta}$). Measurement of $B_\theta(r)$ allows the current density profile, $j(r)$, to be calculated from the B_θ field distribution which gives the local ohmic heating rate and effective charge, Z_{eff} .

Following the first successful measurements of the electron temperature distribution in TOKAMAKS using laser beam scattering, Peacock et al⁽²⁾, it has been the aim of the authors to bring magnetic fields within the set of plasma parameters which can be measured by this technique, since it uniquely offers high spatial and temporal resolution without perturbing the plasma.

It was shown theoretically by Salpeter^(3,4) that the magnetic field influences the scattered light spectrum only when the differential wave vector $\vec{k} = \vec{k}_s - \vec{k}_o$, Fig. 1b, is nearly perpendicular to the local magnetic field vector, \vec{B} . When this condition is satisfied the spectrum is frequency modulated with peaks separated by the electron cyclotron frequency, ω_{ce} . In this paper we exploit the sensitivity of the depth of modulation to the angle between

\vec{k} and \vec{B} . Due to the way in which the ohmic currents $j(r)$ are distributed through the plasma, the magnetic fields and their pitch angle, ϵ illustrated in Fig. 1, vary with plasma radius. Numerically $\epsilon = \arcsin B_\theta/B_T$ where $\vec{B}_T = \vec{B}_\theta + \vec{B}_\phi$. In TOKAMAKS, the toroidal field B_ϕ can be set with considerable accuracy ($\leq 1\%$) so that the pitch angle $\epsilon(r)$ is the quantity of immediate interest.

Measurement of the radial variation in pitch angle in the present study is based on the detection of those particular scattering planes, i.e. planes defined by the directions of the incident and scattered light, which feature frequency modulation of the spectrum.

Unfortunately, in low density, $n_e \approx 10^{19} \text{ m}^{-3}$, high temperature, $T_e \approx 1 \text{ keV}$, plasmas as in TOKAMAKS, the scattered light flux in the individual harmonics is too weak to be recorded directly. We overcome this difficulty by using light collection optics and a Fabry Perot dispersion system which 'multiplexes' the harmonic content to a detectable level. The Fabry Perot allows the angular information in the dispersed spectrum to be related to the variation of field line pitch angle with radius of the plasma column.

Other experimental studies of the location of magnetic surfaces in TOKAMAKS have been reported recently. Alladio and Martone⁽⁵⁾ have determined a local current density by measurements of the displaced Gaussian scattered spectrum. In high temperature TOKAMAKS such a measurement is difficult because of the low ratio of the drift to thermal speed for the electrons, typically $v_d/v_e \approx 0.03$. Non-scattering methods include second harmonic generation at the upper hybrid frequency in the ST TOKAMAK, Cano et al⁽⁶⁾ and the location of q surfaces by collimated neutral deuterium beams traversing the ATC TOKAMAK, Goldston et al⁽⁷⁾. Yet another technique by McCormick et al⁽⁸⁾,

involves the detection of σ and π components of the Zeeman-broadened emission lines from a neutral lithium beam which is directed through the plasma.

THEORETICAL BACKGROUND, THE INFLUENCE OF MAGNETIC FIELD ON THE SPECTRUM OF SCATTERED LIGHT

When the scale length, k^{-1} , of the scattering geometry, as defined by the laser wavelength and scattering angle, is much less than the plasma Debye length, λ_D , only uncorrelated motions of the scattering electrons are represented in the Doppler broadened scattered spectrum. A single electron in the presence of a magnetic field will gyrate about a field line so the velocity component in the \vec{k} direction will vary sinusoidally in time at the gyro frequency $\omega_{ce} = \frac{eB}{m_e}$. If the radius of gyration exceeds the scale length the frequency modulated scattered spectrum will be a sequence of lines separated by the gyro frequency. The detailed spectrum of light scattered by an ensemble of electrons in a magnetised plasma has been calculated by Lehner and Pohl⁽⁹⁾

$$S(k, \omega, \psi) = \frac{1}{\pi \sqrt{z} k v_e \sin \psi} \sum_{n=-\infty}^{+\infty} e^{-n^2/z} \exp \left[- \left(\frac{\Delta \omega - n \omega_{ce}}{k v_e \sin \psi} \right)^2 \right]$$

where $z = k^2 r_L^2 \cos^2 \psi$ and ψ is the angular deviation from perpendicularity of the scattering vector \vec{k} to the field \vec{B} . It consists of a series of Gaussian peaks of width $2 k v_e \sin \psi$, separated by the gyro frequency, Fig. 2. The peaks are bounded by a Gaussian of $2 k v_e$ width, limiting their number to approximately $2 k v_e / \omega_{ce}$ (or $2 k r_L$, where r_L is the Larmor radius). Clearly, when $k \sin \psi v_e \approx \omega_{ce}$ the modulation will disappear which shows the critical dependence of the effect on the orthogonality angle ψ . A factor of two change in the ratio of these two quantities i.e. $\frac{k \sin \psi v_e}{\omega_{ce}}$, may cause the degree

of modulation to change from about 90% to 15%⁽⁹⁾. In the present experiment with a ruby laser the angle ψ has to be less than 0.5° for modulation to be observed. Other practical factors such as the finite acceptance cone of the scattered light and the variation in magnetic fields over the scattering volume will contribute to demodulation⁽¹⁰⁾.

Recently Carolan⁽¹¹⁾ has pointed out that for high temperature plasmas smearing of the peaks will occur at large values of $\Delta\omega = (\vec{k}_s - \vec{k}_o) \cdot \vec{v}_e$. He defines a useful parameter $\gamma = (k_o v_e^2 \sin^2 \theta / 2) / c \omega_{ce}$, where for $\gamma \leq 1$ demodulation at high frequency shifts is not serious. In practical terms this means selecting as small a scattering angle θ as is compatible with the other sources of demodulation. In our case a nominal scattering angle of 30° was used, resulting in $\gamma \approx 0.7$.

EXPERIMENTAL BACKGROUND

Experimental evidence of modulated scattered light spectra from relatively dense ($n_e \approx 10^{22} \text{ m}^{-3}$) plasma has been reported by Evans and Carolan⁽¹²⁾, Kellerer⁽¹³⁾ and Ludwig and Mahn⁽¹⁴⁾, who succeeded in resolving individual gyro peaks. However, in TOKAMAK discharges with typical densities of $n_e = 10^{19} \text{ m}^{-3}$ there are too few scattered photons to allow for the detection of individual peaks.

Sheffield^(15,16) proposed an elegant solution to this problem by which the harmonic content of the scattered light spectrum is multiplexed, i.e. effectively adding up all the peaks. Physically this entails setting the free spectral range, ω_{FSR} , of a Fabry Perot interferometer equal to the gyro peak spacing, ω_{ce} . If smearing of the multiplexed harmonics is to be avoided it is necessary that this matching is achieved with an accuracy better than the reciprocal of

the number of peaks that will be detected i.e. 0.6% in the present experiment.

Inherent in the proposal, is the fact that the scattering directions containing modulated light can be identified as 'bright-up' spots in azimuth of the Fabry Perot fringe, Fig. 4. The scattered spectrum exhibits modulation in only one plane, defined by the scattering geometry and field direction. The intersection of the plane and the Fabry Perot ring pattern results in a partial fringe, which is measured as an azimuthal angle ' μ '. The Fabry Perot has advantages such as high throughput and retention of the angular information i.e. the disposition of the partial fringes.

The interpretation of the azimuthal fringe shift ' μ ' in terms of magnetic field direction is given in a generalised treatment by Carolan⁽¹⁷⁾, that holds for all scattering arrangements and plasma field configurations. An illustration of this, suitable for TOKAMAK application, is shown in vector form in Fig. 3. When the scattered light is scanned along the laser beam the wave vector plane, containing the modulated spectrum, rotates about the laser beam direction due to the B_0 variation (see also Fig. 1b). Two examples are shown, with and without a B_0 field component; the cones represent collected scattered light directions. In the case where $B_0 = 0$ the 'bright-up' of the fringes occur in the plane LOA; when B_0 is finite they appear in LOA'. It can be seen that for larger values of the scattering angle θ the plane of modulated light gives larger values of azimuthal angles, μ_{S1} and μ_{S2} , for the same B_0 field. Since azimuthal information is preserved unaltered in the detection optics, these azimuthal angles will be represented in the partial interference fringes of the Fabry Perot interferometer (cf Fig. 4).

CONSTRAINTS ON THE EXPERIMENT

Various physical effects can broaden the width of the individual spectral peaks. A complete description of the scattering process, for electrons in a magnetic field, which includes all the relevant parameters is not yet available. As the success of the present experiment rests on the simple theory, outlined above, it suffices for our purposes to show that the conditions chosen were within its validity range. The relevant constraints are listed below together with the experimental values in parenthesis, [].

- 1) The bandwidth of the instrumental profile, obtained from the convolution of the laser line profile and the Fabry Perot transmission profile, must be much less than the peak spacing

$$\left[\omega_{ce} \approx 3.5 \times 10^{11} \text{ rad s}^{-1}, \Delta\omega_{\text{laser-F-P}} \approx 4 \times 10^{10} \text{ rad s}^{-1} \right].$$

- 2) The broadening of the spectral peaks introduced by the range of directions of the magnetic field and incident light must be much less than ω_{ce} . Investigations of this problem^(10,18,19) have shown that if the range of \vec{k} and \vec{B} is such that $2 v_e \vec{k} \cdot \vec{B} \leq B \omega_{ce}$ the peak broadening is small compared to ω_{ce} . This criterion has been used⁽¹⁷⁾ in calculating the limits imposed on the incident laser beam divergence $\beta \leq \frac{\omega_{ce}}{2k_o v_e} \left[\frac{\omega_{ce}}{2k_o v_e} = 1.7 \text{ mrad}, \beta = 2 \text{ mrad} \right]$ and the range of field variations in the scattering volume

$$\left| \Delta B_\theta - \Delta B_\varphi \frac{B_\theta}{B_\varphi} \right| \leq \frac{\omega_{ce} B_\varphi}{k_o v_e} \frac{1}{\sin \theta} \cdot \left[\left| \Delta B_\theta - \Delta B_\varphi \frac{B_\theta}{B_\varphi} \right| = 5 \text{ mT}, \frac{\omega_{ce} B_\varphi}{k_o v_e \sin \theta} = 14 \text{ mT} \right].$$

- 3) The electrons must execute a number of complete orbits (≥ 10) within the scattering volume; this requires $\frac{2\pi r_L}{d_s} \ll 1$ (d_s = scattering volume thickness) $\left[\frac{2\pi r_L}{d_s} = 0.04 \right]$.

- 4) The dispersed light from the Fabry Perot etalon must have sufficient intensity and contrast to differentiate experimentally between modulated and unmodulated spectra. This requires the utili-

sation of as many of the spectral peaks as possible due to the small number of photons per peak. The factors limiting the number of useful peaks available are (a) the range of field intensities⁽¹⁷⁾ within the scattering volume $\frac{\Delta B}{B_0} \leq \frac{1}{kr_L} \left[\Delta B/B_0 = 2 \times 10^{-3} \right]$, (b) the smearing effect arising from modulation of \vec{k} due to $k_s \neq k_0$ ⁽¹¹⁾ for large electron velocities $\gamma = k_0 v_e^2 \sin^2(\theta/2)/c \omega_{ce} \leq 1$ $[\gamma = 0.7]$. When both of these criteria are met the light will be modulated to frequency shifts of at least kv_e , i.e. at least 80% of the total intensity of the scattered spectra is deeply modulated.

5) Long range coulomb collisions suffered by an electron gyrating about a force line can perturb its orbit to such a degree that smearing of the scattered spectrum occurs. The role of collisions has been investigated theoretically by several authors^(20,21,22). According to theory, the effect of collisions becomes serious when the random phase error introduced into the scattered light, in one gyro period, becomes a significant fraction of 2π . Since the total phase change experienced by light scattered by a gyrating electron, in a gyro-period, is typically $kr_L \times 2\pi$, the cumulative effect of many long range coulomb encounters becomes important long before a 90° deflection of the electron has occurred (i.e. a 'collision'). The various theories can be summarized by stating that the scattered spectrum will be modulated provided $(kr_L)^2 v_e / \omega_{ce} \leq \alpha$. For 75% modulation, calculations based on, say, the theory of Farley⁽²⁰⁾ gives $\alpha = .05$ while Peratt's⁽²²⁾ calculations suggest $\alpha = 2$. (v_e is the Spitzer⁽²³⁾ electron collisional frequency). Experimental evidence^(12,13,14) shows that the role of collisions has been somewhat over-estimated which suggests values of $\alpha > 2$. $\left[(kr_L)^2 v_e / \omega_{ce} \approx 1 \times 10^{-2} \right]$.

THE SCATTERING EXPERIMENT ON DITE TOKAMAK

The DITE TOKAMAK⁽²⁴⁾ was operated in plasma conditions which gave the optimum parameters for detecting the modulated spectrum. Values of electron temperature, plasma density and toroidal field were $T_e \simeq 350$ eV, $n_e \simeq 2 \cdot 10^{19} \text{ m}^{-3}$, $B = 2$ T. The observation time was set at 70 msec from current zero, when there was a low level of X-ray activity and electrical diagnostics indicated a stable plasma. At this relatively low temperature the number of gyro peaks that need to be superposed is reduced. A nominal scattering angle of 30° was chosen as the best compromise between experimental accuracy and the various smearing effects.

The experimental arrangement is shown schematically in Fig. 4, it includes novel selection optics that utilises a resonant Fabry Perot-prism combination to provide spatial resolution and high optical efficiency. The laser, interferometer and fringe detection system are mounted on a very stable trolley and the laser input and collection optics together with the laser dump are attached to the torus module. The output of an Apollo Q-switched ruby laser (output 10 joules in 15 ns) is deflected into the vertical axis by a prism and reduced by an inverted telescope to a parallel 1 cm diameter beam (divergence 1.2 mrad) which passes through the magnetic axis of the TOKAMAK. Stringent measures are taken to keep the stray light level low i.e. by collimating light absorbing baffles on the input and an efficient laser dump. This was necessary as the detection system was designed to have maximum throughput and is consequently of low contrast. Scattered light is collected through a re-entrant window 75 mm diameter, which is level with the torus wall but 8.5 cm behind the plasma limiter. Situated directly behind the window is an array of

four anti-reflection coated prisms, cut so that each takes light from a known scattering volume and the set as a whole produces near paraxial rays on their output faces. A convex lens projects these rays onto a focal plane stop. Referring to Fig. 4 it can be seen how the rays from the outer prisms are more convergent than those from the centre prisms. This difference in angles together with a 15 times expanding telescope is used to force the light into two predetermined interference fringe orders. Each half of each order then has a spatial correspondence with the scattering volume selected by the prisms. The spatial resolution, ≈ 5 mm, is determined by the back projection of the partial fringe into the scattering column.

The inclination of the field lines varies with radial position. In Fig. 3 it is shown how the plane containing the modulated spectra moves across the collection port. It is therefore important to position the collection prisms to intercept this plane. An estimate of the position of these planes is made from a nominal B_θ distribution and relying on the relatively large prism aperture ($\pm 15^\circ$) to cover any deviation from this estimated position. Crossed wedge prisms are used to compensate for the displacement of the collection prisms to ensure the light passes through the focal plane stop.

A 15 nm interference filter is used to isolate the scattered light before it is matched into the Fabry Perot. The latter has an effective aperture of 13.5 cm and is dielectrically coated to give 70% reflectivity at 694.3 nm, a finesse of 9, i.e. designed for high transmission rather than contrast. The etalon spacing is set to 2.72 mm, by optically contacted pads, which matches the free spectral range to the gyro frequency for a 2 T field. (For high stray laser

light conditions a high reflectivity coating can be used and the etalon spacers matched to $2\omega_{ce}$ to tune out the 694.3 nm light). A convex lens focuses the fringe system on the extended red photocathode of a gated (50 ns) image tube RCA 73435 AK. This is fibre optic coupled to a three stage intensifier RCA 8606 which gives a luminous gain of $3 \cdot 10^5$. A video camera, an EMI intensified Ebitron, is used to record the intensified partial fringes on magnetic tape. The recorded pattern is displayed on a TV monitor for processing. An earlier experiment by Forrest, Muroaka and Peacock⁽²⁵⁾ estimated a basic system sensitivity of 18 photoelectrons per degree of azimuth; the number of scattered photoelectrons here is expected to be 60 to 150 per degree of azimuth.

The first pre-aligned prism array, is designed to accept scattered light from the magnetic axis, 6 and 10 cm above the axis. The toroidal field was varied in increments until partial fringes were first observed indicating the matching condition was satisfied. Three distinct sets of fringes, for example Fig. 5a, were obtained while on other shots correlation was necessary to distinguish the 'bright-ups' from noise spots; the stray light was not detectable. To ensure the 'bright-up' spots coincided with the selected Fabry Perot orders, reference fringes were induced, by tapping some light off the laser beam, in lieu of stray laser light. As the quality of these was poor due to exposure problems they have been drawn in for clarity. As a check the plasma current was reversed, this tilts the field lines and hence the plane containing the modulated light in the opposite direction. In this case partial fringes were only present from the two prisms looking at the magnetic axis, Fig. 5b. This is as expected because no prisms were positioned to intercept

the tilted planes. As a further test the TOKAMAK was run with both the plasma current and toroidal field reversed and again the four 'bright-ups' were observed.

To complete a radial scan a second prism array was used; here the prisms were set to look on the magnetic axis and at 4 cm, 15 cm and 21 cm above the axis. Partial fringes were again observed but this time with a different azimuthal dispersal, Fig. 5c.

From the video data the azimuthal shifts were related to field inclination angles and as B_ϕ is known, B_θ for each selected radial position is calculated, Fig. 6a. This profile represents a gas current I of 135 kA, while the measured current was 130 kA.

From this poloidal field distribution, $B_\theta(r)$, we derive a 'q' profile. This is compared with $q(r)$ calculated from the electron temperature profile obtained by previous scattering measurements under similar plasma conditions, Fig. 6b, where it is assumed the current density $j \propto T_e^{\frac{3}{2}}$ so that

$$q(r) = \frac{2\pi r^2 B_\phi}{\mu_0 R I} \frac{\int_0^a T_e^{\frac{3}{2}} r dr}{\int_0^r T_e^{\frac{3}{2}} r dr}$$

ACCURACY OF THE TECHNIQUE

The purpose of the diagnostic is to measure the magnetic field direction in the toroidal co-ordinates of the TOKAMAK device. The field direction is measured in the scattering geometry co-ordinates and then from the orientation of these with respect to the machine, the magnetic field vector in toroidal co-ordinates can be calculated. Accuracy in determining the former depends on the sensitivity of the directions of modulated scattered light on the field directions: the greater the scattering angle the more sensitive the dependency⁽¹⁷⁾.

An estimate of the accuracy by which the field direction can be measured is obtained from the product of the sensitivity and the range of scattering directions where the light is modulated. For $\theta = 30^\circ$, $T_e = 350$ eV, the ratio B_θ/B_ϕ can be measured with an accuracy $\Delta(B_\theta/B_\phi) = 0.3\%$. The problem of orientating the laser beam and detection optics to the torus was alleviated by the precision machining of the diagnostic port faces. Before fitting the prism array to the torus, it was set up on a test rig and back projection of an expanded helium-neon laser beam indicated a spatial accuracy of ± 2 mm in centering the selected scattering volumes. Our measurements depended on the location of the azimuthal position of the partial fringes on a video system. Examination of this basic data, Fig. 5 shows this is somewhat subjective, but it appears possible to determine the angular positions μ to within 0.4° . This is equivalent to determining the field line inclination to within 0.15° or a $\Delta q < 5\%$ which is close to the basic theoretical accuracy of the method.

CONCLUSIONS

Our conclusions can be summarised as follows. Magnetic field profiles can be measured by light scattering from the free electrons in TOKAMAKS causing no perturbation to the plasma medium. Basically the method involves detection of the modulation in the scattered light spectrum due to cycloidal motion of the electrons around the field lines.

The sensitivity of the modulation to the perpendicularity condition ($\vec{k} \perp \vec{B}_T$) ensures a high degree of accuracy in determining the pitch of the magnetic field line i.e. to within 0.15° .

We have demonstrated a detection system that magnifies small

changes in the pitch angle of magnetic field lines. The sensitivity has been optimised by using as large a scattering angle as is consistent with conditions for modulation to be satisfied. It has also been shown that the criteria required to observe modulation, in the present experiments, lie within the validity of simple theory.

An extension of the technique to future TOKAMAKS seems promising.

It is a pleasure to acknowledge the pioneering work and continued support from D.E. Evans, J. Sheffield and J. Katzenstein. The successful application of the technique to TOKAMAKS is due to considerable help and advice from J. Hugill and J.W.M. Paul and the support of the DITE diagnostic and operations group.

REFERENCES

- (1) Shafranov, V.D., Sov. Phys. Tech. Phys. 15, 2, 175-182 (1970).
- (2) Peacock, N.J., Robinson, D.C., Forrest, M.J., Wilcock, P.D., Sannikov, V.V., Nature 224, No 5218, 448-490 (1969).
- (3) Salpeter, E.E., Phys. Rev. 120, 1528-1535 (1960).
- (4) Salpeter, E.E., Phys. Rev. 122, 1663-1674 (1961).
- (5) Alladio, F. and Martone, M., Phys. Lett. 60A, 39-41 (1977).
- (6) Cano, R., Fidone, I. and Hosea, J.C., Phys. of Fluids 18, 1183-1186 (1975).
- (7) Goldston, R.J., Mazzucato, E., Slusher, R.E. and Surko, C.M., Plasma Physics and Controlled Nuclear Fusion Research, (Proc. 6th IAEA Conf. Berchtesgaden, 1976) I, 371-383 (IAEA Vienna, 1977).
- (8) McCormick, K., Kick, M. and Olivain, J., 8th European Conf. on Controlled Fusion and Plasma Physics, Prague (1977).
- (9) Lehner, F. and Pohl, F., Z. Physik 232, 405-414 (1970).
- (10) Carolan, P.G. and Evans, D.E., Plasma Physics 13, 947-975 (1971).
- (11) Carolan, P.G., IPP KFA Jülich Internal Report No 1474 (1977), 13th Conf. Phen. in Ionised Gases, Berlin (1977), paper submitted to Plasma Physics.
- (12) Evans, D.E. and Carolan, P.G., Phys. Rev. Lett. 25, 1605-1608 (1970).
- (13) Kellerer, L., Z. Physik 232, 415-417 (1970).
- (14) Ludwig, D. and Mahn, C., Phys. Letters A, 35A, 191-197 (1971).
- (15) Sheffield, J., Plasma Physics, 14, 385-395 (1972).
- (16) Sheffield, J., Plasma Scattering of Electromagnetic Radiation, Academic Press, 54-59 (1975).
- (17) Carolan, P.G., Plasma Physics 19, 757-775 (1977).

- (18) Carolan, P.G. and Evans, D.E., Proc. 10th Conf. Phen. in Ionised Gases, 533 Oxford (1971).
- (19) Meyer, R.L. and Leclert, G., Nuclear Fusion 12, 269-271 (1972).
- (20) Farley, D.T., J. Geophys. Res. 69, 197-200 (1964).
- (21) Dougherty, J.P., Phys. Fluids, 7, 1788-1799 (1964).
- (22) Peratt, A.L., Phys. Fluids 18, 57-66 (1975).
- (23) Spitzer, L., Physics of Fully Ionized Gases, Interscience Publishers, (1972).
- (24) Paul, J.W.M., et al, Proc. of 6th IAEA Conference on Plasma Physics and Controlled Fusion Research, Berchtesgaden (1976), Vol 2, 269.
- (25) Forrest, M.J., Muroaka, K. and Peacock, N.J., Proc. 11th Conf. Phen. Ionised Gases, Prague, 5.3.3. (1973).

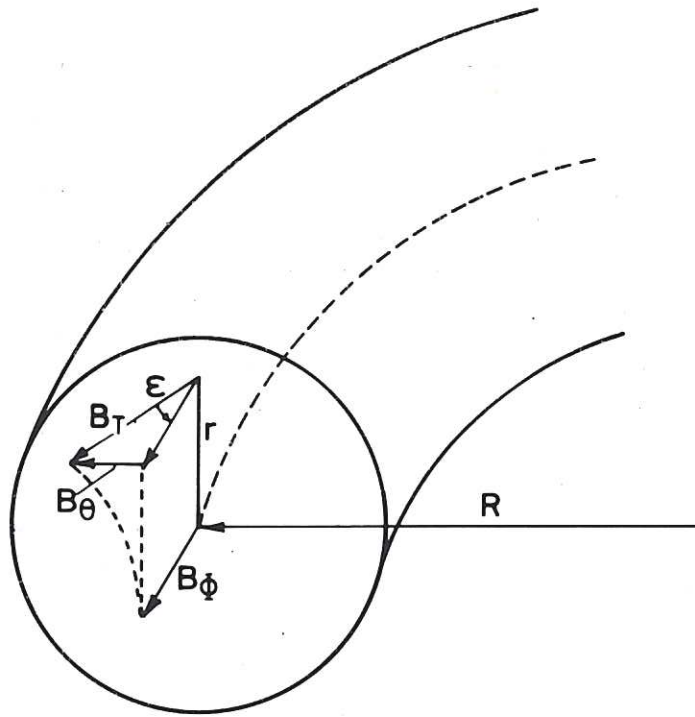


Fig.1a The magnetic field configuration in a TOKAMAK.

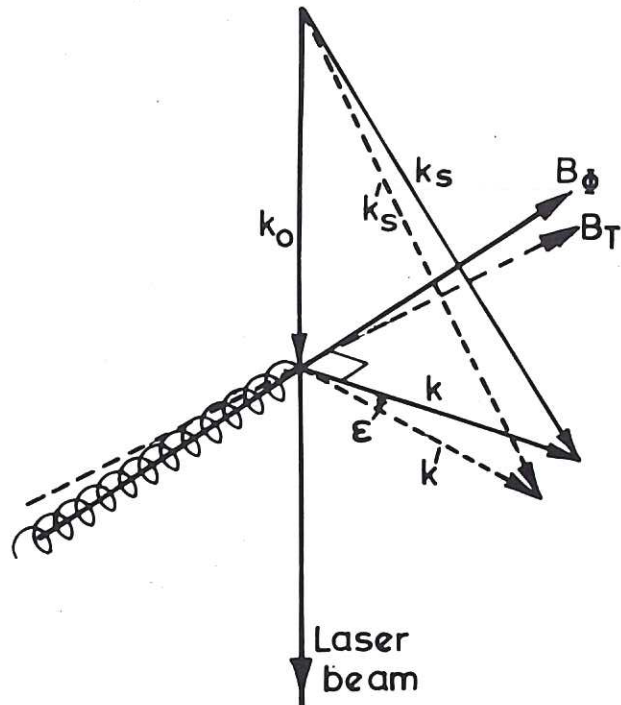


Fig.1b Vector diagram for scattering in a magnetic field. Two cases are shown (a) Full lines show situation where there is no B_θ field i.e. on the magnetic axis, (b) Dotted lines indicate how the wave vector plane rotates as B_θ assumes finite values.

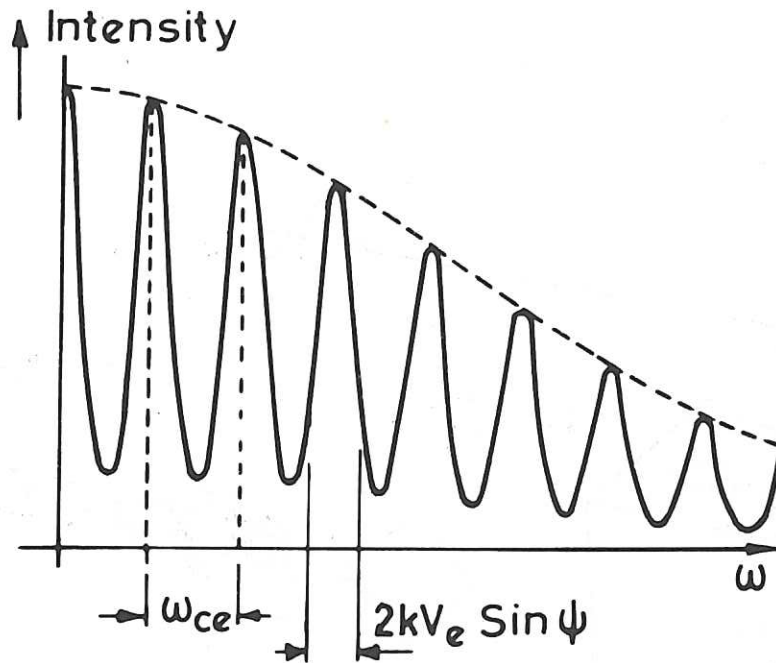


Fig.2 Scattered spectrum for a magnetised plasma for \vec{k} perpendicular to \vec{B} .

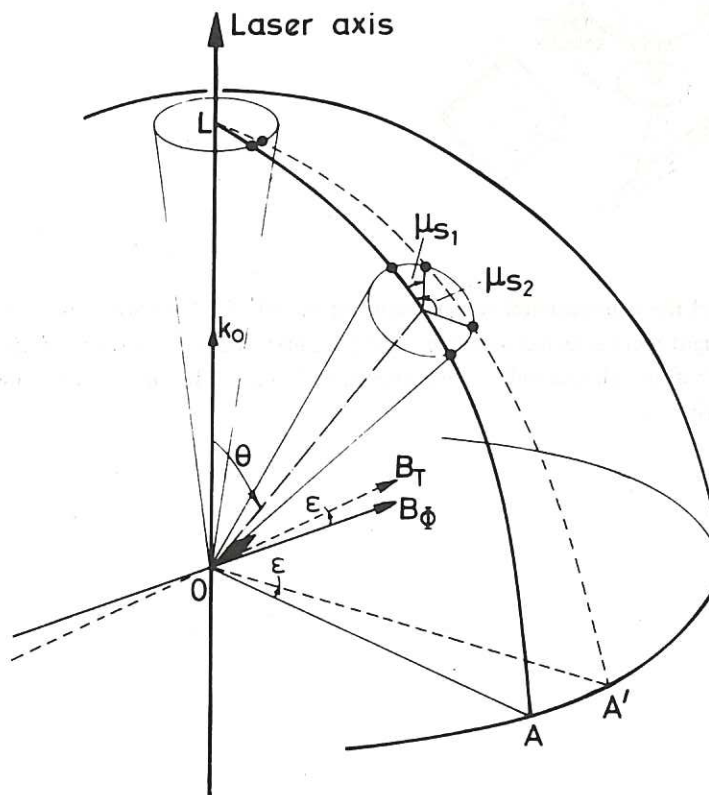


Fig.3 Optical magnification of the inclination angle of field lines. The modulated spectrum in the plane perpendicular to the magnetic axis is contained in LOA. For a field line tilted by angle ϵ the modulation is in plane LOA'. The intersection of these planes and the collection aperture is equivalent to the locus of the partial Fabry Perot fringes. It can be seen how the sensitivity increases with the larger scattering angle. $\vec{B}_T = \vec{B}_\phi + \vec{B}_\theta$.

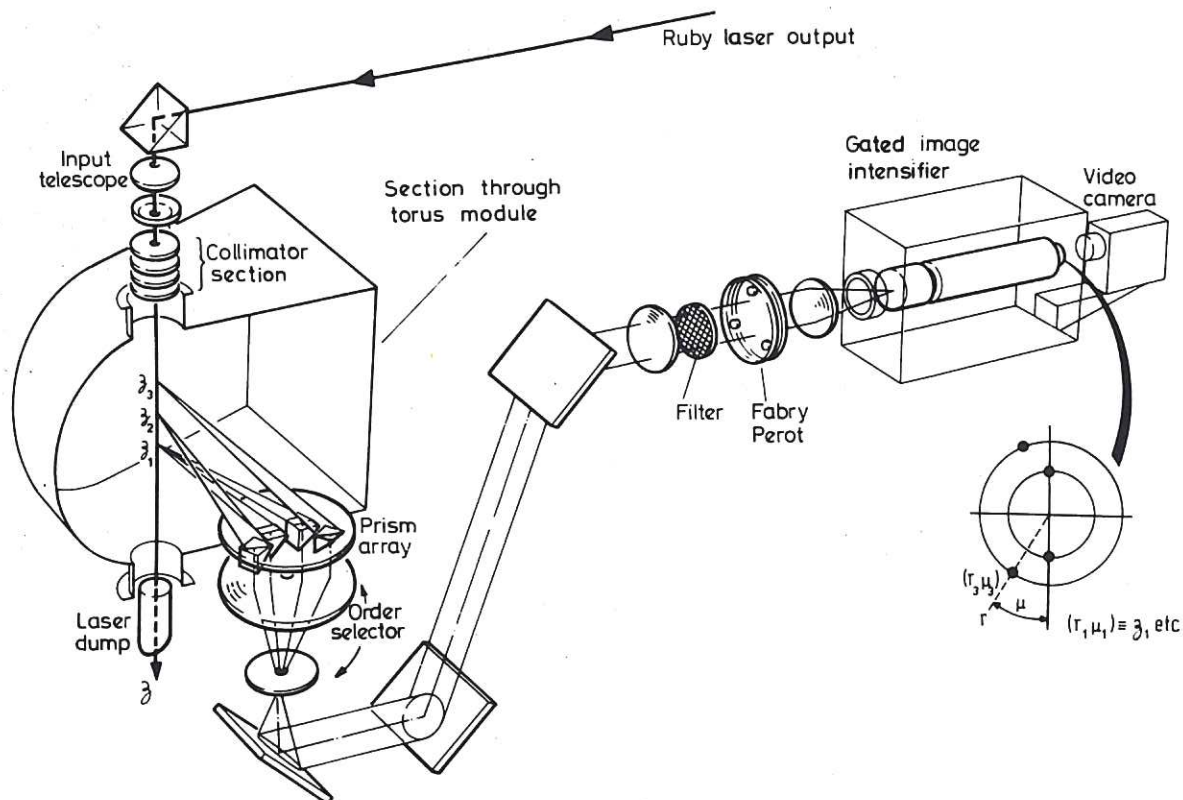


Fig.4 Schematic of the experimental arrangement on the DITE TOKAMAK module. The four prisms that collect scattered light from selected positions along the laser beam are shown. Variations in \vec{B} at different positions z_1, z_2 etc along plasma radius corresponds to different 'bright-up' positions (r_1, μ_1) (r_2, μ_2) etc on the Fabry Perot fringe pattern.

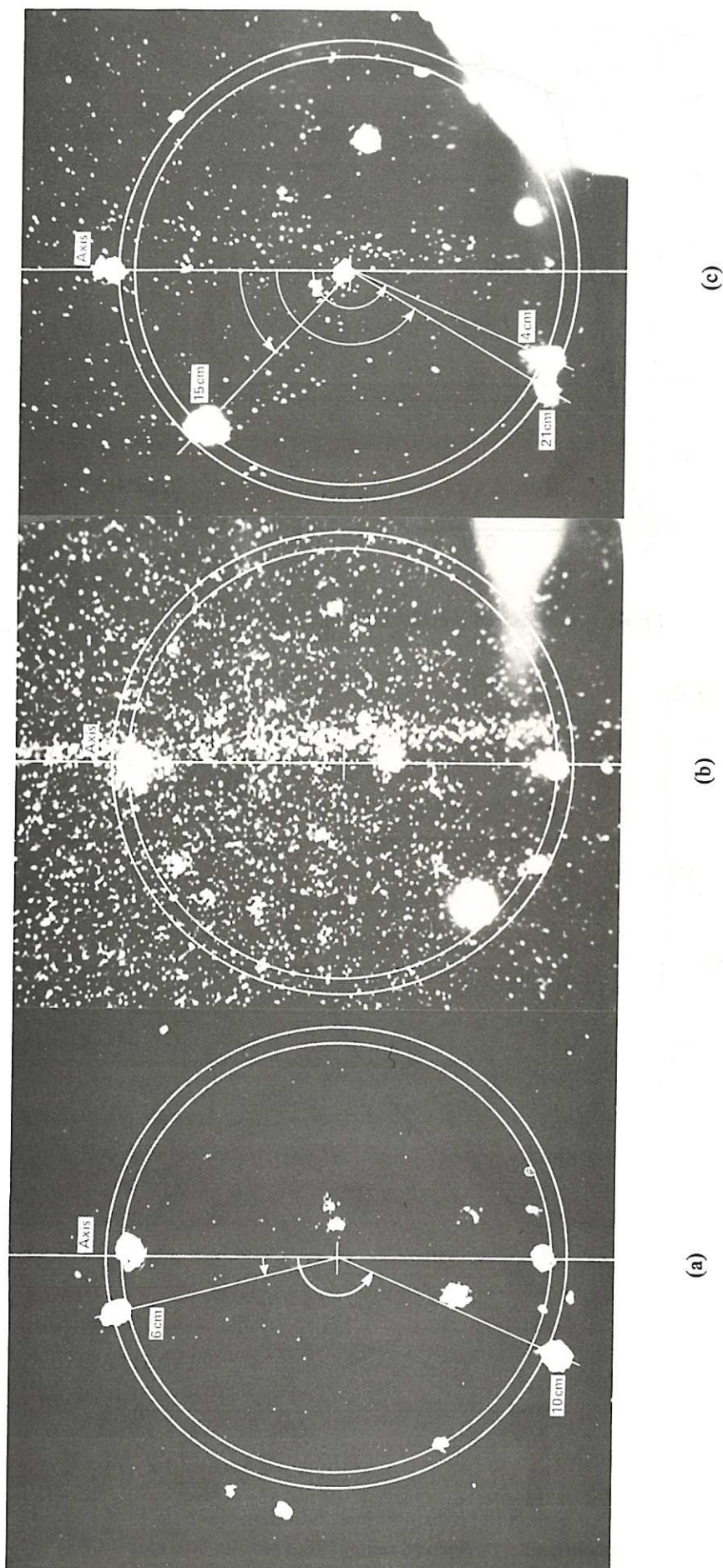


Fig.5 Video output data showing intensified partial Fabry Perot fringes labelled with their spatial correspondence. The circular reference fringes are drawn in for clarity. (a) First prism array, (b) First prism array with plasma current reversed, (c) Second prism array, plasma current and toroidal field reversed. The background noise on (a) and (c) has been suppressed by reducing the brightness of the video system.

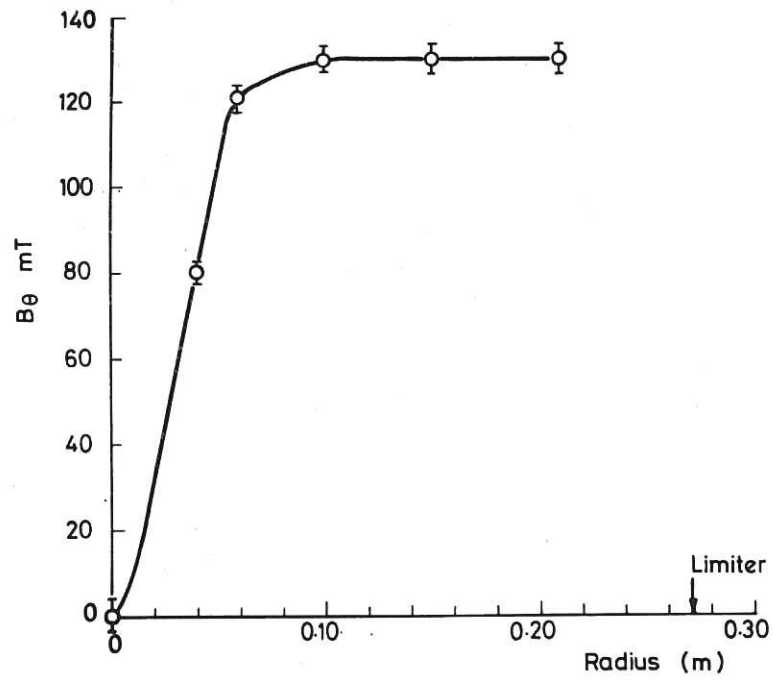


Fig.6a The measured poloidal field $B_\theta(r)$ distribution.

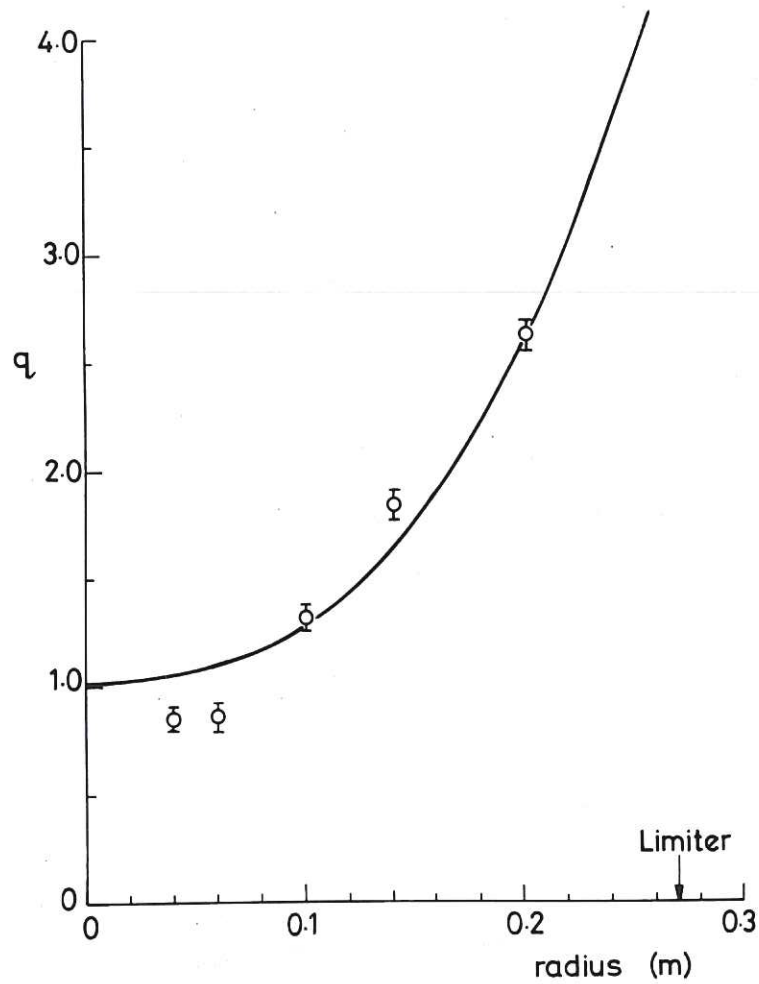


Fig.6b Comparison of 'q' distributions, \odot from poloidal field measurements and — electron temperature profiles assuming $j \propto T_e^{3/2}$ and constant Z_{eff} in similar plasma conditions.

1. The first part of the document discusses the importance of maintaining accurate records of all transactions and activities. It emphasizes that proper record-keeping is essential for transparency and accountability, particularly in the context of public administration and financial management. The text outlines various methods for collecting and organizing data, including the use of standardized forms and digital databases.

2. The second part of the document focuses on the role of technology in improving efficiency and reducing errors. It highlights the benefits of using software solutions for data entry, storage, and analysis. The text also addresses the challenges associated with implementing new technologies, such as the need for staff training and the potential for data security breaches. Recommendations are provided for selecting appropriate software and ensuring its secure use.

3. The third part of the document discusses the importance of regular audits and reviews. It explains that audits are necessary to verify the accuracy of records and to identify any discrepancies or irregularities. The text describes the different types of audits, such as internal audits and external audits, and provides guidance on how to conduct them effectively. It also emphasizes the importance of maintaining a clear audit trail and documenting all findings and actions taken.

4. The fourth part of the document addresses the issue of data privacy and security. It discusses the legal requirements for protecting personal and sensitive information and provides practical advice on how to implement security measures. The text covers topics such as access control, data encryption, and regular security updates. It also emphasizes the importance of educating staff about data security and the potential consequences of a breach.

5. The fifth part of the document discusses the importance of communication and collaboration. It explains that effective communication is essential for ensuring that all stakeholders are aware of the requirements and procedures. The text provides guidance on how to develop clear communication plans and how to foster a culture of collaboration and teamwork. It also emphasizes the importance of regular reporting and updates to keep everyone informed of the progress and any issues that arise.

6. The sixth part of the document discusses the importance of continuous improvement. It explains that processes and procedures should be regularly reviewed and updated to reflect changes in requirements and technology. The text provides guidance on how to conduct regular reviews and how to implement improvements. It also emphasizes the importance of documenting all changes and the reasons for them.

7. The seventh part of the document discusses the importance of training and development. It explains that staff should be regularly trained and updated on the latest requirements and procedures. The text provides guidance on how to develop training programs and how to evaluate their effectiveness. It also emphasizes the importance of providing opportunities for staff to develop their skills and knowledge.

8. The eighth part of the document discusses the importance of documentation. It explains that all procedures, policies, and records should be clearly documented and easily accessible. The text provides guidance on how to develop and maintain a comprehensive documentation system. It also emphasizes the importance of ensuring that all documentation is up-to-date and accurate.

9. The ninth part of the document discusses the importance of compliance. It explains that all activities must comply with relevant laws, regulations, and standards. The text provides guidance on how to ensure compliance and how to handle any non-compliance issues. It also emphasizes the importance of keeping up-to-date with changes in requirements and standards.

10. The tenth part of the document discusses the importance of transparency and accountability. It explains that all activities should be clearly documented and reported to the relevant stakeholders. The text provides guidance on how to develop and maintain a transparent reporting system. It also emphasizes the importance of being open and honest about any issues or challenges that arise.